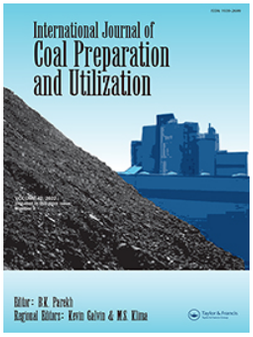

International Journal of Coal Preparation and Utilization

ISSN: (Print) (Online) Journal homepage: https://www.tandfonline.com/loi/gcop20

Development of a circulating fluidized bed partial gasification process for co-production of metallurgical semi-coke and syngas and its integration with power plant for electricity production

Diyar Tokmurzin, Desmond Adair, Timur Dyussekhanov, Kalkaman Suleymenov, Boris Golman & Berik Aiymbetov

To cite this article: Diyar Tokmurzin, Desmond Adair, Timur Dyussekhanov, Kalkaman Suleymenov, Boris Golman & Berik Aiymbetov (2022) Development of a circulating fluidized bed partial gasification process for co-production of metallurgical semi-coke and syngas and its integration with power plant for electricity production, International Journal of Coal Preparation and Utilization, 42:3, 899-924, DOI: 10.1080/19392699.2019.1674842

To link to this article: https://doi.org/10.1080/19392699.2019.1674842

INTERNATIONAL JOURNAL OF COAL PREPARATION AND UTILIZATION
2022, VOL. 42, NO. 3, 899–924
https://doi.org/10.1080/19392699.2019.1674842

Taylor & Francis
Taylor & Francis Group

Development of a circulating fluidized bed partial gasification process for co-production of metallurgical semi-coke and syngas and its integration with power plant for electricity production

Diyar Tokmurzin[a], Desmond Adair[a], Timur Dyussekhanov[b], Kalkaman Suleymenov[b], Boris Golman[a], and Berik Aiymbetov[c]

[a]School of Engineering, Nazarbayev University, Astana, Kazakhstan; [b]Department of Research & Development, Research & Development Engineering Center of ERG, Astana, Kazakhstan; [c]Laboratory of Green Energy and Environment, National Laboratory Astana, Astana, Kazakhstan

ABSTRACT

Coal, coke, and semi-coke are currently irreplaceable materials in the iron and steel industry. Coal is converted to coke or semi-coke in fixed bed coke-ovens which have many drawbacks and cause environmental damage. A novel method for the production of semi-coke using circulating fluidized bed partial coal gasification is experimentally studied. The method involves a fast devolatilization stage which promises to reduce the effect on the environment compared to conventional coke-ovens. Experiments are conducted with high volatile Shubarkol coal in a custom-made atmospheric reactor consisting of a riser, a cyclone, a loop seal, and equipped with a semi-coke withdrawal system. The reactor is operated autothermally, at temperatures varying from 700°C to 1000°C. The coal feed rate varies from 40 to 70 kg/h, with a particle size distribution up to 20 mm. During the experiments, char samples are withdrawn from the riser and the standpipe. The samples have a volatile content of 3-6%, carbon content above 85%, high structural strength (92.64%), low bulk density (270 kg/m^3) and high porosity (28.4%) compared to conventionally produced semi-coke. It is confirmed that even using the laboratory scale setup it is possible to produce up to 0.367 kg of semi-coke per kg of coal.

ARTICLE HISTORY
Received 10 April 2019
Accepted 27 September 2019

KEYWORDS
Circulating fluidized bed; partial gasification; semi-coke; fast devolatilization; high volatile coal

Introduction

Economic growth and urbanization are increasing the demand for the expansion of energy and water supply, transportation, housing, and public facilities. This leads to a growing demand for steel and its alloys. World demand for steel has almost tripled since the 1970s (World steel Association, 2018), and the main driver of this trend is Asia, where steel production almost quadrupled between 1970 and 2017 (IEA 2017; World Coal Institute 2007). Currently coal, coke, and semi-coke are irreplaceable in the iron and steel industry. Conventionally, steel is produced in blast furnaces, where coke is used as a vital component that plays the role of a reducing agent and heat source, and, provides mechanical strength to burden and permeability to gas and liquid phases (Li et al. 2014a). Coke is made by heating

CONTACT Diyar Tokmurzin dtokmurzin@nu.edu.kz School of Engineering (Rm 2227), Nazarbayev University, 53, Kabanbay batyr Ave., Astana, 010000, Kazakhstan.

Color versions of one or more of the figures in the article can be found online at www.tandfonline.com/gcop.

coking coals in a coke oven in a reducing atmosphere. High prices for coking coals and their scarcity have led steelmaking companies to search for ways to reduce coke consumption, alternative raw materials, alternative steel smelting, and coke making processes. Recently developed commercial processes such as iron bath smelting (American Iron and Steel Institute 2010; Street et al. 1998), blast furnaces with coal injection (Tang et al. 2017), COREX/FINEX process (Menéndez, Álvarez, and Pis 1999; Tang et al. 2017), and ferroalloys production (Hasanbeigi, Arens, and Price 2014; Xu and Cang 2010) allow the fine fraction semi-coke to be substituted for coke as the reducing agent. Semi-coke is a coal char with high-fixed carbon and low volatile content produced from coal through pyrolytic devolatilization.

Semi-coke production implies the devolatilization of carbonaceous materials such as coal and is currently carried out through the heating of coal in a coke oven with no oxygen supply. When volatiles are driven out of coal, coke is ejected from coke oven batteries and extinguished with water in order to avoid its combustion in the open air. Semi-coke typically has a volatile content of 10% or less (Li et al. 2016) and fixed carbon content on a dry basis not less than 70% (Zhu et al. 2015), and, it consists of particles between 0 and 8 mm in diameter (Li et al. 2016; Strakhov 2009).

The conventional semi-coke production process suffers from several notable disadvantages, including (i) release of thermodynamically unstable coal volatiles, which undergo conversion to syngas containing gas and tar during heating (Pan et al. 2015), with tar being a source of contamination of soil and water by tar and environmentally harmful phenol compounds, (ii) production of the wet product after water quenching, which subsequently requires additional energy for drying before use of semi-coke in carbothermic processes, and (iii) high capital cost of treatment and utilization facilities of coke-oven gas (He and Wang 2017). The development of a novel semi-coke production technology described in the present paper was partly motivated by the desire to overcome the above limitations. Moreover, semi-coke is currently produced in industry using 20–80 mm coal fraction, and a fine fraction of 0–20 mm is separated from the coal particle mixture as unsuitable for processing, which leads to economic losses. Therefore, the utilization of fine fraction coal for semi-coke production can further increase the economic attractiveness of the newly developed technology.

On entering a circulating fluidized bed (CFB) gasifier, a coal particle undergoes fast heating and gasification, which consists of three consecutive stages namely drying, devolatilization (pyrolysis), and gasification. Devolatilization is the stage when volatile matter of solid fuel is removed. It is a very important stage, especially in the case of high volatile solid fuels. (Pan et al. 2015; Gonenc et al. 1990; Trubetskaya et al. 2016) Pyrolysis in a stationary bed of conventional coke oven is considered as slow pyrolysis because of low heating rates of less than 1°C/s. Devolatilization during CFB partial gasification can be considered as fast pyrolysis, due to high heating rates reaching some 1000°C/s (Pan et al. 2015; Sermin et al. 1990; Trubetskaya et al. 2016). Devolatilization in the fluidized bed at high temperatures and high heating rates demonstrates improved devolatilization efficiency and reduced tar yield (Borah, Ghosh, and Rao 2011). Tar contains contaminants such as phenols, polycyclic aromatic hydrocarbons, and ammonia. Therefore, technologies utilizing fluidized bed could be promising for the production of high-quality semi-coke with low environmental impact.

Unlike coal partial gasification, production of semi-coke using coal pyrolysis has attracted the attention of many researchers (Fushimi et al. 2017; Hu et al. 2011; Song, Liu, and Wu 2016; Wootten et al. 1988; Wu et al. 2017b). Production of semi-coke was

also a subject of process simulation studies, where essentially char gasifiers and combustors played the role of a heat source for separate atmospheric allothermal pyrolizers (Dai et al. 2017; Guo et al. 2014; Jing et al. 2017; Yi et al. 2013). These studies were implemented using process integration and simulation methods in ASPEN PLUS software. Such integration of polygeneration processes, in general, allow the reduction of CO_2 emissions, CO_2 recovery costs, or overall efficiency (Hu et al. 2011).

Even though the circulating fluidized bed (CFB) process is a rapidly developing and extensively studied technology for combustion and gasification of coal, petroleum coke, biomass, and waste derived fuels, coal partial gasification has not been studied extensively. CFB reactors possess considerable versatility due to a high overall rate of gasification process driven by an enhanced heat and mass transfer, and a long residence time of the char due to char recirculation and resulting in low char loss (Alauddin et al. 2010; Basu 1999; Nowak and Mirek 2013). Very few studies have investigated the coal partial gasification in a CFB, and they mainly presented the results on the thermodynamic analysis of the CFB (Nowak and Mirek 2013), development of co-production systems of hydrogen and electricity (Li et al. 2014b; Xu et al. 2012) or reported bench scale allothermal CFB experiments (Ye et al. 2017). Ye et al. conducted their experiments in an H_2O-O_2 (Ye et al. 2017) and CO_2-O_2 (Ye et al. 2018, 2017) atmosphere using an externally heated lab-scale CFB reactor with a cylindrical riser 120 mm in diameter and 2600 mm in height. Their study was conducted in the relatively limited temperature range of 885–980° C, using the narrow range of fine coal particles of 0.35–0.9 mm in diameter. The carbon conversion rate was between 79% and 92% in steam-O_2 and between 78% and 88% in CO_2 -O_2 partial gasification. Ye et al. (Ye et al. 2018, 2017) have also studied partial gasification char properties, using Raman spectroscopy, Fourier-transform infrared spectroscopy (FTIR), and scanning electron microscopy (SEM). Raman spectroscopy and FTIR showed that steam-O_2 partial gasification results in a loss of different functional groups in char, and, chars become more ordered and less reactive (Ye et al. 2018). SEM revealed that CO_2 -O_2 partial gasification of coal results in increased porosity inside the chars. Ye et al. also observed that in case of CO_2-O_2 gasification chars become more disordered as the gasification temperature increases (Ye et al. 2017).

Reactivity is considered as one of the important characteristics of semi-coke that is used to evaluate its performance in a blast furnace and in COREX process (Menéndez, Álvarez, and Pis 1999). Semi-coke intrinsic properties, such as carbon crystallite size, ash content, and ash catalytic effect, influence the reactivity of semi-coke (Zhang 2018). These properties depend on parent coal properties and heat treatment conditions. In this research carbon, crystallite structure is studied using an X-ray diffraction (XRD). XRD is a powerful tool for the determination of the crystalline characteristics of carbonaceous materials, including semi-coke (Lu et al. 2001). For instance, Wu and Sahajwalla investigated the influence of carbon structure, carbon content and sulfur content on coal dissolution in molten iron and discovered that the crystallite size has a critical effect on the carbon dissolution (Wu and Sahajwalla 2014). Taylor concluded that the temperature of the coal heat treatment has a critical influence on the transformation of the random and disordered network connections found in coal to an ordered hexagonal structure with higher crystallinity (Taylor 2000). Conventionally, semi-coke is produced in fixed-bed low-temperature ovens (400–600°C), and coke is produced at higher temperatures (reaching 1100°C) and demonstrate higher

crystallinity as found by XRD analysis (Xu et al. 2018). In contrast, CFB partial gasification takes place at intermediate temperatures between 700°C and 1000°C. Thus, there is a need to investigate the effect of heat treatment of semi-coke produced by partial gasification of high volatile Shubarkol coal in the CFB reactor at intermediate temperature.

A novel method involving the thermal-oxidative fast pyrolysis with partial gasification of coal in the CFB for semi-coke production is examined in the present paper. In this paper, the semi-coke production process is investigated in an autothermal larger scale CFB reactor, over a wider temperature range from 700°C to 1000°C, using the coal with wider size distribution of 0–20 mm and of a lower carbon conversion compared to recent studies by Ye et al. (Ye et al. 2017). Use of coal CFB partial gasification for semi-coke production allows to avoid integration of the allothermal pyrolytic process and the heat source. Physical and chemical characteristics of semi-coke produced during the experiments are examined in order to provide characteristics necessary for industry. Another important feature of the proposed process is the decision to avoid the use of sand as a bed material. The dense-phase-zone in the riser and in the loop seal is formed of char. This is motivated by the intention to retain the highest possible carbon content of the bulk withdrawn material. XRD analysis is used for investigation of the heat treatment effect on semi-coke reactivity. Additionally, the novel partial gasification CFB reactor is proposed to be integrated with a Rankine cycle power plant.

The primary objective of this study is to prove experimentally the feasibility of circulating fluidized bed technology for autothermal production of char suitable for use as a metallurgical semi-coke and investigate the potential to integrate the semi-coke production process with a thermal power plant using the fine fraction of coal. Such an approach and integration allows for the improving of energy efficiency and environmental performance, eliminating the necessity of coke-oven gas treatment. A secondary objective of this study is to optimize the operating conditions of the CFB process to maximize devolatilization and minimize conversion of fixed carbon.

Materials and Methods

Materials

High volatile Shubarkol coal was used in this study as the main raw material. It is mined from open-pit mines in the Central Kazakhstan region. The coal with size 0–20 mm was fed into the reactor.

Standard Coal Analysis

The coal feedstock characteristics such as particle size distribution (PSD), proximate analysis, ultimate analysis, and calorific value are required for a CFB process design and operation (Kunii and Levenspiel 1997; Yang 2003). This data is also essential for quantitative evaluation of the process efficiency, identification of opportunities to integrate a semi-coke production plant with a power plant, and quantification of the power output that can be produced from a unit of coal input.

To determine the PSD, coal was first sieved through a 20 mm hand sieve, then three representative samples were extracted using a coning and quartering procedure. Then, the representative samples were sieved with an automatic sieving machine (AS200, Retsch) using sieves having mesh sizes of 10, 8, 6, 4, 2, 1, and 0.5 mm. The standard analysis of the coal samples was conducted including proximate analysis and ultimate analysis. Coal samples for proximate and ultimate analyses were coned and quartered and then ground and sieved through a 200 μm sieve. The proximate analysis was conducted in triplicate using a thermogravimetric analyzer (TGA Q500, TA instruments). The heating rate of the TGA was set to 20°C/min and with the maximum temperature at 900 °C. Samples for the ultimate analysis were dried at 105°C for 12 h and then analyzed using a CHNS analyzer (Variocube, Elementar), also in triplicate. The calorific value of the coal was determined using a bomb calorimeter (B-08MAK, Etalon). The ash fusion temperature was measured by the pyramid cone method according to the ASTM D1857 standard in an ash fusion determinator (5E-AF400, CKIC).

Semi-coke Characterization

In order to compare semi-coke from the partial gasification process with that obtained from the conventional process and rotary drum furnace process, semi-coke samples were characterized for properties required by the industry (Commitee of technical requilation and metrology, Ministry of industry and new technologies 2011; Svyatov, Strakhov, and Surovtseva 2012). Moisture content, ash content, volatiles content, and fixed carbon content were determined using the thermogravimetric analyzer. Sulfur content was determined using the CHNS analyzer.

Samples porosity, specific total pore volume and specific surface area were measured by the nitrogen absorption technique using an automated gas sorption analyzer (Autosorb, Quantochrome instruments). Before analysis 200–300 mg of semi-coke was degassed for 8 h at 350°C in order to clean the surface of the sample. Adsorption and desorption isotherms were measured and interpreted by the Brunauer-Emmett-Teller (BET) method (Brunauer, Emmett, and Teller 1938).

The semi-coke bulk density was determined according to the GOST 54251–2010 standard which corresponds to ISO 567:1995 ("GOST R 54251 Coke – Determination of Bulk Density in a Small Container (ISO 567:1995)" 2012). The GOST 9521–2017 standard was selected for structural strength analysis of semi-coke and for comparison the obtained results with literature data (Commitee of technical requilation and metrology, Ministry of industry and new technologies, Republic of Kazakhstan 2011; Svyatov, Strakhov, and Surovtseva 2012). Chlorine content was determined according to GOST 9326–2002 standard ("GOST 9326–2002 Solid Mineral Fuels – Determination of Chlorine" 2002) using a method of burning the sample in a calorimetric bomb.

Semi-coke Intrinsic Properties

Carbon crystallite structure was determined using the X-ray diffraction method. The method needs a relatively large amount of solid sample that can be obtained by simple quartering. This enabled average measurements from the sample in order to determine the bulk powder characteristics rather than local characteristics of separate particles. This is

important for heterogeneous materials such as coal, coke, or semi-coke. X-ray diffraction analysis allows to determine the crystalline parameters such as crystallite size and its distribution (Crystallite diameter – L_a, crystallite stacking height – L_c, interlayer spacing – d_{002}). Semi-coke samples were milled, sieved through a 0.075 mm sieve, and then analyzed using a Rigaku SmartLab® X-ray diffractometer (XRD) with Cu-Kα radiation source (35 kV, 28.5 mA). Scanning of samples was conducted with 2θ in the range from 10 to 100 degree at scanning rate of 1 deg/min. The shape of the carbon peak was used for determining the crystalline size.

Experimental Setup

To validate the feasibility of the proposed method, the experiments were conducted in a custom-designed CFB reactor. Figure 1 illustrates a schematic diagram of the experimental setup. The CFB system consisted of a riser, standpipe, loop seal, coal supply system, gas-solid separators, sample withdrawal devices and syngas treatment subsystem. The riser (1) was made of heat-resistant stainless-steel tube with an inner diameter of 150 mm and a height of

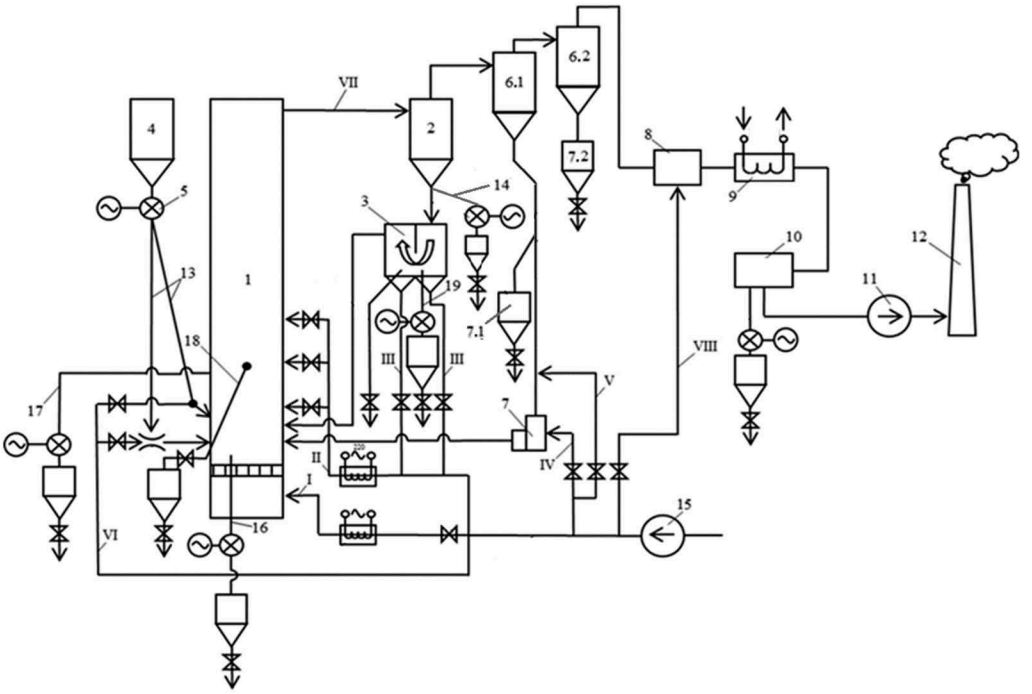

Figure 1. Schematic diagram of experimental setup: 1. Riser; 2. Cyclone; 3. Loop seal; 4. Bunker; 5. Screw feeder; 6.1 Sanitary cyclone; 6.2 Sanitary cyclone; 7.1 Cyclone bunker; 7.2 Cyclone bunker; 8. Combustor; 9. Heat exchanger; 10. Bag filter; 11.exhaust fan; 12. Chimney; 13. Two hoses for coal supply; 14. Semi-coke extraction line from the standpipe; 15. Air blower; 16. Semi-coke extraction line from the riser bottom; 17. Semi-coke extraction line from the top of the dense-phase-zone; 18. Manual semi-coke extraction line from the top of the dense-phase-zone; 19. Semi-coke extraction line from the bottom of the dense phase zone; I – primary air; II – secondary air; III – air to loop seal chambers; IV – air blow to L-valve; V –air stream for aeration of standpipe; VI – air stream for pneumatic transport of coal; VII – syngas from the reactor; VIII – air stream for syngas afterburner.

5.6 m. The fluidizing air (I) from an air blower (15) was injected into riser through a series of bubble caps fixed on the air distribution plate at the bottom of the riser. Coal from a bunker (4) was introduced into the riser through one of two hoses (13), both of 70 mm in inner diameter. The coal inlets were located at distances of 700 mm and 350 mm from the air distribution plate. The coal flow rate was adjusted with a screw feeder (5).

Syngas evolved in the reactor and char particles entrained with gas were transported to a cyclone (2), where the gas was separated from the particles. The particles collected in the cyclone (2) were conveyed through a standpipe (14) to a loop seal (3). The loop seal was made of two bubbling fluidized bed chambers, receiving and conveying. The secondary air was injected through the bubble caps located at the bottom of chambers. The height of both chambers was 600 mm. The receiving chamber had a rectangular cross-sectional area of 80 mm × 80 mm, and the conveying chamber 120 mm × 80 mm. Char from the receiving chamber passed to the conveying chamber and then was recycled to the riser (1).

Syngas was supplied from the exhaust cyclones (6.1 and 6.2) to a combustor (8) and, then, flue gas passed through a cooler (9) and a bag filter (10) to a chimney (12). Particles captured in cyclones were accumulated in bunkers (7.1 and 7.2). The riser, loop cyclone and two exhaust cyclones were fully insulated with 100 mm thick ceramic wool to minimize heat losses. Air and gas streams included: I – primary air, II – secondary air, III – air to loop seal chambers, IV – air blow to L-valve, V – air stream for aeration of standpipe, VI – air stream for pneumatic transport of coal, VII – syngas from the reactor, VIII – air stream for syngas afterburner.

The temperature in the reactor was measured with K-type thermocouples connected to a 12-channel temperature data logger (RMT59, Elemer). Thermocouples were located

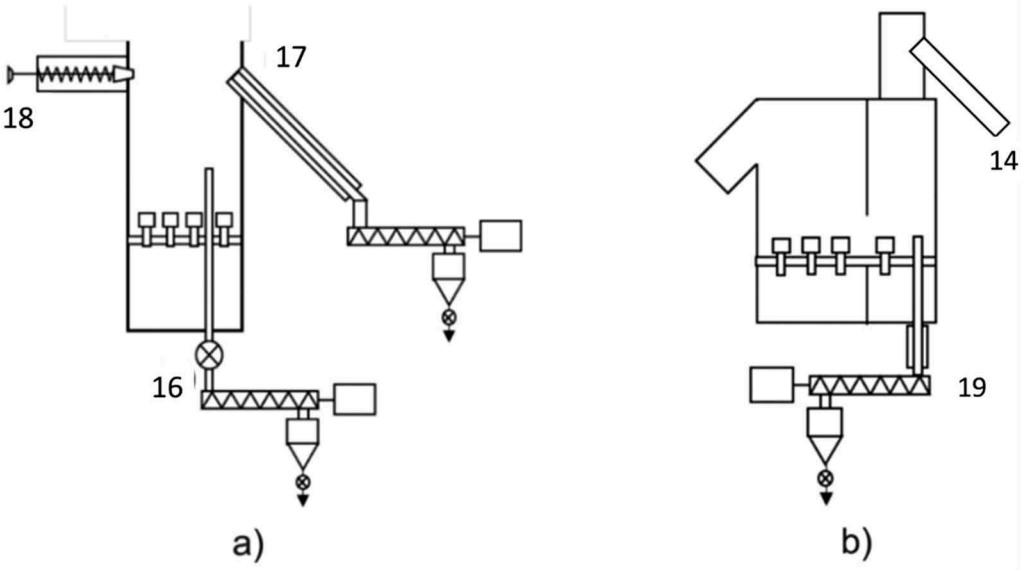

Figure 2. Semi-coke withdrawal ports: a) lower part of the CFB riser section (b) loop seal and standpipe. 16. Semi-coke extraction line from the riser bottom; 17. Semi-coke extraction line from the top of the dense-phase-zone; 18. Manual semi-coke extraction line from the top of the dense-phase-zone; 19. Semi-coke extraction line from the bottom of the dense phase zone.

along the riser column, in the loop cyclone, and in the loop seal. The pressure was measured with pressure transducers (PD100, Owen).

Material extraction mechanisms are described in better details in Fig. 2. The mechanized systems were installed in the lower part of the CFB riser section to collect samples from the top (17) and the bottom (16) of the riser dense-phase-zone, the loop seal (19) and the standpipe (14). The semi-coke samples were also withdrawn manually from the top of the dense-phase-zone (18) by opening a plug that covers a hole in the lower part of the CFB riser.

Reactor Start-up

Typically, CFB gasifiers and combustors operate with inert bed materials in the riser, such as silica sand. In this study, unlike previous partial gasification research (Nowak and Mirek 2013; Xu et al. 2012; Li et al. 2014b; Ye et al. 2017), semi-coke was extracted from the riser and from the standpipe. Such an extraction approach allows for the production of semi-coke of larger sizes, which more valued in the iron and steel industry. However, use of sand in the riser dense-phase-zone and its extraction with semi-coke will increase the semi-coke bulk inert material content. To avoid this, the reactor was started and operated without sand, and the dense-phase-zone char played the role of the heat transfer media. During low air-to-fuel equivalence ratio (ER) partial gasification char can be deliberately accumulated in the dense-phase-zone and its level can easily be estimated based on differential pressure. Considering these factors, experiments were conducted without using sand as the bed material. To startup the experiment, the riser was filled with 2.5–3.0 kg of semi-coke with size of 0–8 mm playing the role of bed material and 2.0–2.5 kg of semi-coke with size of 0–2 mm was added to the standpipe. The primary and secondary air was heated to 600–650°C using an electric heater (13). The coal supply started when the bed temperature reached 300°C, and the significant rise in bed temperature began after the coal ignited at 350°C. At this point the heater was turned off because the reactor in this process was able to operate autothermally. When the temperature reached 800–900°C, the coal feed rate and air supply were set at appropriate values to maintain the desired temperature and subsequently char circulation in the unit was started by supplying secondary air into both chambers of the loop seal.

Reactor Operation

The reactor temperature was varied in the range 700–1000°C and the supply of air was set to keep an ER of 0.19–0.33. The superficial velocity of air at the bottom of the reactor was maintained at 4–5 m/s to ensure the fast fluidization upflow conditions in the riser section with the main parameters measured during the experiments being the fuel feed rate, temperature, air feed rate, differential pressure in the riser and loop seal, and syngas composition. Differential pressure allowed to estimate the height of the dense-phase-zone in the riser. The solid products such as semi-coke and entrained char samples were collected for analysis from the top of dense-phase-zone in the riser and from the standpipe, and entrained particles were collected in two exhaust cyclones. Semi-coke retrieval from the riser was started when the semi-coke material accumulation increased the riser dense-phase-zone height to the height of the screw conveyor junction to the riser. Similarly, retrieval of semi-coke from the standpipe began when solid

material accumulation in the loop-seal and standpipe increased the height of the dense-phase-zone to the height of the screw conveyor junction to the standpipe.

Semi-coke samples were analyzed for PSD and proximate analysis was conducted to evaluate the amount of fixed carbon and the amount of impurities in the form of volatile matter. Char samples were also analyzed for PSD, proximate analysis and calorific value to evaluate char potential as a fuel in the boiler. Operating conditions of eleven experiments are listed in Table 1, these operating conditions are also listed in tables with corresponding results.

Results and Discussion

Standard Coal Analysis

The results of proximate and ultimate analyses of Shubarkol coal used in the present study are summarized in Table 2. This coal has low ash content, high volatile matter content, and high carbon content, compared with other coals. Examples of five other coals proximate and ultimate analyses are given for comparison in Table 2, which include three coals from China (Huating, Yangquan anthracite, and Shenmu), coal from Kazakhstan (High ash Ekibastuz coal), and coal from Russia (Kuznets coal). Yangquan anthracite is used in China for blast furnace injection (Tang et al. 2017). The table also includes Shenmu coke which is made from Shenmu coal and LKSP coke which is made from Kuznets coal (Korshenko et al. 2016; Svyatov, Strakhov, and Surovtseva 2012). As can be seen from the table, Shubarkol coal has proximate and ultimate analyses close to Shenmu and Kuznets coals, but with higher volatile content. Even though Shubarkol coal has low ash, low sulfur, and a high-fixed carbon

Table 1. Operating conditions of the experiments conducted.

Experiment No		1	2	3	4	5	6	7	8	9	10	11
B_{coal}	kg/h	58	44	65	45	45	55	48	48	40	50	50
$V_{air\ total}$	nm^3/h	110	94	94	112	112	112	65	80	94	107	72
T_{bed}	°C	930	950	930	810	880	990	700	850	780	865	890

B_{coal}, coal feed rate; $V_{air\ total}$, total air flow rate; T_{bed}, riser dense-phase-zone temperature.

Table 2. Coal and coke proximate and ultimate analyses.

Sample	W_r, wt %	A_d, wt %	V_{daf}, wt %	FC_r wt%	C_{daf}, wt %	H_{daf}, wt %	N_{daf}, wt %	O_{daf}, wt %	S_{daf}, wt %	NHV, kcal/kg
					Coal					
Shubarkol coal	10.6	4.25	44.5	47.26	76.9	5.35	1.45	15.3	1.0	6334.7
Huating coal[37]	7.6	19.4	18.0	46.39	43.7	2.3	0.9	9.3	0.4	5482.5
Yangquan coal anthracite coal[7]	0.63	9.95	7.06	82.36	83.29	3.31	1.12	6.66	0.62	7705
Ekibastuz coal [50]	5.4	42.0	32.0	37.3	81.5	5.3	1.6	10.9	0.7	4000
Shenmu coal [51]	8.8	4.2	38.0	59.4	82.38	6.37	1.00	9.99	0.26	6379
Kuznets coal [51]	9.0	5.0	41.0	56.1	79.35	5.57	2.40	12.30	0.38	7780
					Coke & semi-coke					
Shenmu coke [51]	1.4	10.9	3.83	85.6	93.24	2.07	1.05	3.38	0.26	-
Kuznets semi-coke LKSP [51]	13.8	10.0	17.2	74.5	88.83	2.97	2.76	5.24	0.20	-

W_r, moisture content on as received basis; A_d, ash content on dry basis; V_{daf}, volatile content dry ash free basis; FC_r, fixed carbon on as received basis; C_{daf}, carbon on dry ash free basis; H_{daf}, hydrogen on dry ash free basis; N_{daf}, nitrogen on dry ash free bsis; O_{daf}, oxygen on dry ash free basis; S_{daf}, sulfur on dry ash free basis; NHV, net heating value.

Table 3. Shubarkol coal ash chemical composition.

Sample	A_d	SiO_2	Al_2O_3	Fe_2O_3	CaO	MgO	TiO_2	MnO	P_2O_5	SO_3	Na_2O	K_2O
Shubarkol coal	4.25	58.1	22.2	7.1	2.7	1.8	1.1	-	0.5	3.4	1.8	1.3
Coal [38]	2.64	13.67	5.7	27.42	32.23	4.46	0.49	0.36	-	13.68	0.95	0.08
Semi-coke [38]	11.42	28.24	18.78	10.95	17.26	2.49	1.26	0.43	-	18.24	0.87	0.10
coke [38]	12.00	46.59	30.00	9.07	6.72	1.48	1.52	1.47	-	1.47	0.73	0.48

A_d, ash content on dry basis.

content comparable with Kuznets and Shenmu coal it does not have the caking properties necessary for coke production (Korshenko et al. 2016). The composition of Shubarkol coal ash is given in Table 3 together with ash content of lump coal, semi-coke, and coke which were analyzed by Zhang et al. (Zhang 2018). Coal ash contains metal oxides, some of which have catalytic effect on gasification reactions. Fe_2O_3, CaO, K_2O, and Na_2O metal oxides with catalytic effect influence solid fuels reactivity (R. S. Xu et al. 2018; Zhang 2018). As it can be seen from the table, Shubarkol coal ash has less Fe_2O_3, CaO, and K_2O compared to other solid fuels.

The coal PSD is given in Table 4, with its particle size in the range of 0 to 20 mm. The coal mean diameter was 2.4 mm and almost half of the coal particles was smaller than 1 mm. Thus, coal used in the present study belongs to the fine particle fraction. Existence of even small quantities of particles with size above 8–10 mm, can cause defluidization and non-uniform temperature distribution in the dense-phase-zone. However, large particles are expected to reduce in size due to fragmentation and attrition. Table 5 summarizes the measured values of deformation temperature (DT), shrinkage temperature (ST), hemisphere temperature (HT), and flow temperature (FT). The ash deformation temperature of Shubarkol coal is above the CFB operating temperatures, which reduces the chance of bed defluidization due to ash agglomeration.

Effect of Air-to-fuel Equivalence Ratio on Bed Temperature

One of the most important parameters of the CFB operation is the bed temperature. Coal gasification is a complex process where multiple homogeneous and heterogeneous reactions take place simultaneously, most of which are endothermic (Ye et al. 2018). Higher temperatures intensify devolatilization of coal and cracking of released tar. One of the aims of this study is to limit heterogeneous solid carbon reactions in order to maximize char output. It is known that the air-to-fuel equivalence ratio significantly influences the bed temperature. Increasing ER instigates a rise of reactor temperature, and the

Table 4. Coal cumulative undersize particle size distribution.

d, mm	0.5	1	2	4	6	8	10	20
Percent passing, %	30.1	47.7	65.5	75.5	84.3	87.4	90.5	100

d, sieve opening size.

Table 5. Coal ash fusion temperature.

Coal	DT (°C)	ST (°C)	HT (°C)	FT (°C)
Shubarkol	1180	1271	1332	1366

DT, deformation temperature; ST, shrinkage temperature; HT, hemisphere temperature; FT, flow temperature.

devolatilization and gasification reactions rates are directly correlated with reactor temperature. Additionally, as it was previously noted by Jing et al., an increase of ER and consequent increase of bed temperature comes at the cost of a reduced syngas heating value (Jing et al. 2017). An increase of air flowrate also increases the gas velocity and the amount of char particles entrained from the reactor dense-phase-zone. Consequently, there is a need to study experimentally the relationship between the bed temperature and ER in order to determine the minimum ER required for maintaining the desired temperature.

Experiments in the present study were conducted by varying the coal feed rate from 50 to 70 kg/h and the ER from 0.19 to 0.33. Figure 3 illustrates the effect of ER on bed temperature. The bed temperature was significantly higher at the high coal feed rate than the one at low feed rate at the same ER value. Moreover, the slope of the straight line fitted to ER versus the bed temperature is slightly higher for the higher coal feed rate than that for the lower feed rate. These tendencies can be explained by the fact that the larger volume of volatiles evolves during feeding coal at higher feed rates. The ER in this study is lower than that during gasification experiments, which typically varies between 0.3 and 0.45 (Yang 2003). Higher ER increases carbon conversion and total syngas gas yield (Chen et al. 2011). In contrary, low ER favors accumulation of char as a bed material. However, during the first experiments, after some time of operation, it was found that large particles began to collect at the bottom of dense-phase-zone and accumulate on the air distribution plate. Accumulation and buildup of the char bed caused the appearance of hot spots close to the reactor bottom where an oxygen-carbon reaction preferably took place. This caused a significant rise of temperature and damage to the reactor, resulting sometimes in burn-outs of the reactor body. To reduce such an effect, the riser bottom was modified from a cylindrical to a conical shape. This allowed for an increase of gas velocity at the bottom of the reactor without increasing the air supply. Considering the typical CFB operating temperature range from 700°C to 1000°C, at a fuel feed-rate from 65 to 70 kg/h, the ER that ensures this temperature range was found to be between 0.19 and 0.25. At

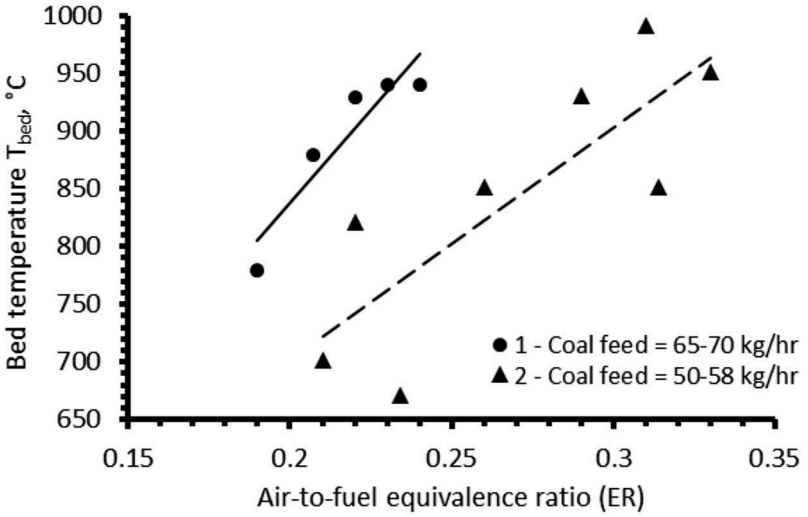

Figure 3. Bed temperature as a function of air-to-fuel equivalence ratio.

a fuel feed-rate from 50 to 58 kg/h, the ER is from 0.21 to 0.31. However, at a higher ER above 0.25 burnout of fixed carbon from semi-coke can be expected.

Effect of Bed Temperature on Semi-coke Carbon Content

Two of the most important characteristics of semi-coke are the carbon content and impurities content. Impurities essentially consist of volatile matter remaining in the semi-coke. During coal devolatilization, coal volatile matter evolves to gas and tar due to thermo-chemical conversion. This study considers the effect of bed temperature on the volatile matter content remaining in the semi-coke. Semi-coke samples were extracted from the top of the dense-phase-zone and standpipe in order to investigate if their volatile content have any difference. Additionally, bed material was collected through a maintenance hatch when the air blower was stopped, and the reactor set for cooling.

Figure 4(a and b) illustrates the effect of bed temperatures on the volatile matter content of the semi-coke withdrawn from the reactor. As can be seen from these figures increasing the bed temperature intensifies devolatilization of coal. Comparison of the best-fit lines revealed that the effects of temperature on semi-coke volatile content in the riser and loop seal were similar. The bulk density of bed material was relatively low at 500–520 kg/m^3. The bulk density of semi-coke removed from the top of the dense-phase-zone was 220–270 kg/m^3, which is significantly less than that of semi-coke from conventional coke-ovens density 960 (Svyatov, Strakhov, and Surovtseva 2012) −1150 kg/m^3 (Kumar et al. 2008). This can be explained by development of coal particles porosity and swelling due to fast devolatilization of high volatile coal. The same phenomena was observed by Yu et al. (Yu et al. 2003) during devolatilization of high volatile coal particles at high heating rates. Similar effect is expected in case of CO_2-steam partial gasification in CFB, Ye et al. (Ye et al. 2017) also reported increased porosity of char samples and the effect strengthened at high operating temperatures in CO_2-steam partial gasification.

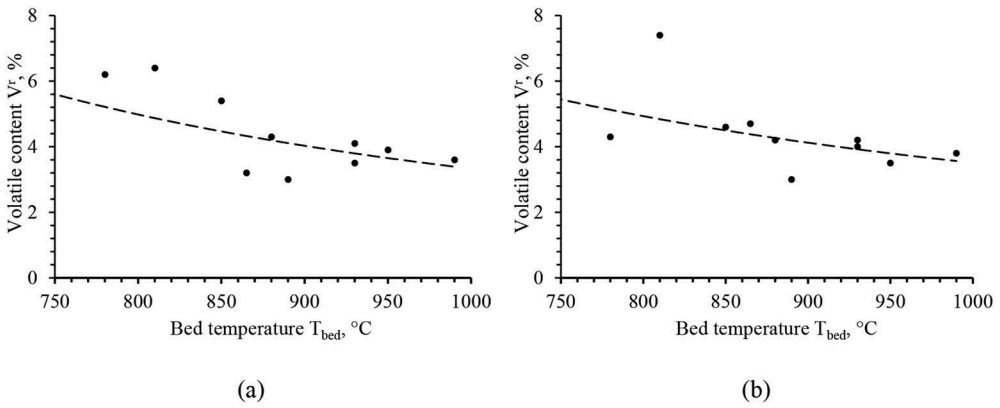

Figure 4. Volatile matter content of semi-coke at various bed temperatures, (a) semi-coke withdrawn from top surface of dense-phase-zone in riser, (b) semi-coke withdrawn from standpipe.

Table 6. Semi-coke proximate analysis.

Experiment No		1	2	3	4	5	6	7	8	9	10	11
B_{coal}	kg/h	58	44	65	45	45	55	48	48	40	50	50
$V_{air\ total}$	nm3/h	110	94	94	112	112	112	65	80	94	107	72
T_{bed}	oC	930	950	930	810	880	990	700	850	780	865	890
Semi-coke withdrawn from the riser												
B_{bed}	kg/h	8.7	5.6	10.8	6	4.8	8.1	6.1	7	6.2	4.5	5.5
W_r	wt.%	1.5	3	3.2	2.1	2.4	2.2	1.5	2.3	2.9	1.8	2
A_{dry}	wt.%	8.8	8.9	10.6	7.7	8.3	8.0	8.2	7.8	7.9	8.1	8.0
V_{dry}	wt.%	4.2	4.0	3.6	6.5	4.4	3.7	5.5	5.5	6.4	3.3	3.1
FC_{dry}	wt.%	87.0	87.1	85.7	85.8	87.3	88.3	86.3	86.7	85.7	88.6	89.0
Semi-coke withdrawn from the standpipe												
$B_{standpipe}$	kg/h	9.1	9.1	9.7	8.4	11.7	9.5	8.8	8.4	5.3	6.5	4.9
W_r	wt.%	3.3	3	3.2	2.5	1.9	2.1	3	2.7	3	3	2
A_{dry}	wt.%	9.0	8.9	10.6	7.7	8.3	7.8	8.4	7.8	7.9	8.2	8.0
V_{dry}	wt.%	4.1	3.6	4.3	7.6	4.3	3.9	5.9	4.7	4.4	4.8	3.1
FC_{dry}	wt.%	86.9	87.5	85.0	84.7	87.5	88.4	85.8	87.5	87.6	86.9	89.0

B_{coal}, coal feed mass flow rate, $V_{air\ total}$, total air flow rate; T_{bed}, riser dense-phase-zone temperature; B_{bed}, mass flow rate of semi-coke withdrawn from the riser dense-phase-zone; W_r, moisture content on received basis; A_{dry}, ash content on dry basis; V_{dry}, volatiles content on dry basis; FC_{dry}, fixed carbon content on dry basis; $B_{standpipe}$, mass flow rate of semi-coke withdrawn from the standpipe.

Table 6 provides proximate analysis on as received basis and dry basis of material withdrawn at various experiments and corresponding operating conditions. All the material in the reactor was dry due to the high operating temperatures. During withdrawal of samples, they were cooled in the screw transporter covered with a cooling jacket, thus avoiding wet quenching. The semi-coke samples are hygroscopic, and their moisture content is entirely adsorbed from the atmosphere. Therefore, to provide a better understanding, the ash, volatile matter and fixed carbon content are given in Table 6 on a dry basis. In general, the results of the semi-coke proximate analysis are in agreement with industry requirements for semi-coke produced in conventional coke-ovens as described in Table 7. At an operating temperature above 850°C, the volatile content of semi-coke was below 5%. This well correlates with fast devolatilization experiments such as wire mesh reactor (WMR) (Ra et al. 2014). In an experimental CFB reactor, the coal inlet and semi-coke withdrawal point were located close to each other, which caused some not yet devolatilized particles to be withdrawn alongside with devolatilized semi-coke. The effect of the distance between coal inlet and semi-coke outlet was tested during the reactor operation by switching off the semi-coke outlet screw (17)

Table 7. Comparison of semi-coke produced using three different methods.

Characteristic	CFB partial gasification (this study, experiment 5 is taken for comparison)	Rotary drum furnace [45]	Coke-oven furnace [46]
$W_{r,}$ wt.%	2.4	1.94	<12
A_{dry} wt. %	8.3	4.73	<8
$V_{daf,}$ wt.%	4.3	6.56	<6
FC_{dry}, wt.%	87.5	89	-
Bulk density, kg/m^3	270	961	-
Structural strength, %	92.64	74.1	>75
Chlorine content Cl_d, %	0.03	-	<0.1
Sulfur content, S_d%	0.34	-	<1
Arsenic content As_d	-	-	<0.01
Reactivity with CO_2, cm^3/g s	-	4.10	>2 cm^3/g s
Nitrogen porosity, %	28.4	24.5	-

W_r, moisture content on received basis; A_{dry}, ash content on dry basis; V_{daf}, volatile content dry ash free basis; FC_{dry}, fixed carbon content on dry basis; Cl_d, chlorine content on dry basis; As_d, arsenicum content on dry basis.

during feeding coal. When the dense-phase-zone height increased over the outlet (17), coal supply was switched off and simultaneously semi-coke extraction screw was switched on. Expectedly this reduced the volatile matter of the semi-coke. On an industrial scale the distance between coal inlet and semi-coke outlet is expected to be bigger.

Table 7 summarized measured results related to the quality of obtained semi-coke such as bulk density, structural strength, total pore volume, chlorine content, sulfur content, reactivity with CO_2, arsenic content, and nitrogen porosity. For comparison purposes, the data on semi-coke produced in a rotary drum furnace (Svyatov, Strakhov, and Surovtseva 2012) and the requirements of the national standard for semi-coke manufactured using the coke-oven furnace (Commitee of technical requilation and metrology, Ministry of industry and new technologies, Republic of Kazakhstan 2011) were added to Table 7. As can be seen from Table 7, semi-coke produced in this study has characteristics that meet or exceed other two examples. CFB semi-coke has higher structural strength, higher porosity, and lower bulk density. Structural strength of coke and semi-coke depends on hardness and thickness of the pores walls. Swelling and development of porosity of coal particles with increased structural strength during devolatilization suggests that pore walls are strengthened due to increased crystallinity of carbon structure in semi-coke.

Comparison of proximate analysis characteristics of semi-coke given in Table 7 and Yangquan anthracite proximate analysis given in Table 2 suggests that the semi-coke produced in this study using the CFB reactor can be used for blast furnace injection.

Size Distribution of Semi-coke

Figure 5(a) illustrates the results of PSD analysis of semi-coke collected in the riser dense-phase-zone, and semi-coke added to the riser at the start of each experiment. The coal feed PSD was added for comparison purpose. Particles with sizes distributed between 4 and 10 mm formed the bed in the dense-phase-zone. Coal with sizes from 0 to 20 mm was fed through screw feeders after heating up the reactor. Larger particles were subjected to cracking and

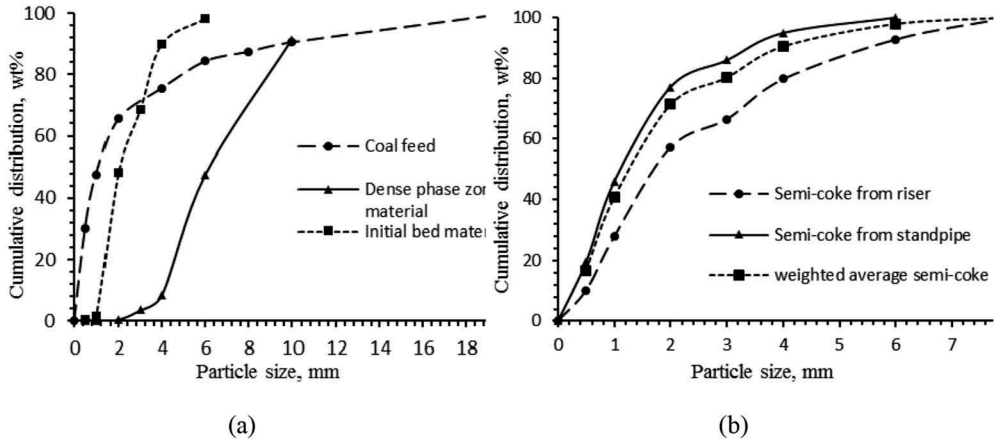

Figure 5. Size distribution of particles circulating in reactor: (a) materials in riser including coal feed, dense-phase-zone and initial char bed, (b) semi-coke from riser, standpipe, and weighted average semi-coke collected in experiment No. 5.

attrition, whereas the smaller particles were entrained and either gasified, recirculated through loop seal or entrained out of the reactor alongside with syngas. The narrow fraction of semi-coke from 0 to 6 mm was used to generate the bed in the riser at the start of experiments.

Figure 5(b) shows the size distribution of semi-coke withdrawn from the reactor riser, standpipe, and their weighted average in experiment No. 5. The particles collected in the riser were of a slightly larger size with wider size distribution than the ones withdrawn from the standpipe. The particle size distribution is an important characteristic related to semi-coke applicability for certain metallurgical processes. For instance, typically, 0–6 mm semi-coke is used for production of silicomanganese. For production of ferronickel, ferrosilicon, calcium carbide and other ferroalloys, semi-coke with a larger particle size (6–18 mm) is utilized. As the raw coal particles were smaller than 20 mm, it was not possible to produce semi-coke of 6–18 mm size in the present experiments. Most of the semi-coke from the standpipe had a size below 4 mm and 77% had a size smaller than 2 mm. Semi-coke from the riser had coarser PSD, 92.8% of particles were in the range of 0–6 mm, with the remaining 7.2% were in the range of 6–8 mm. As can be seen in Table 6, the amount of semi-coke withdrawn from the riser was not equal to the one collected in the standpipe and both amounts varied in different experiments. As a result, the weighted average PSD of two samples was also varied and 98% of particles lied in the 0–6 mm range. This semi-coke can be used for blast furnace injection (Tang et al. 2017) which can result in reduced coke and coal consumption.

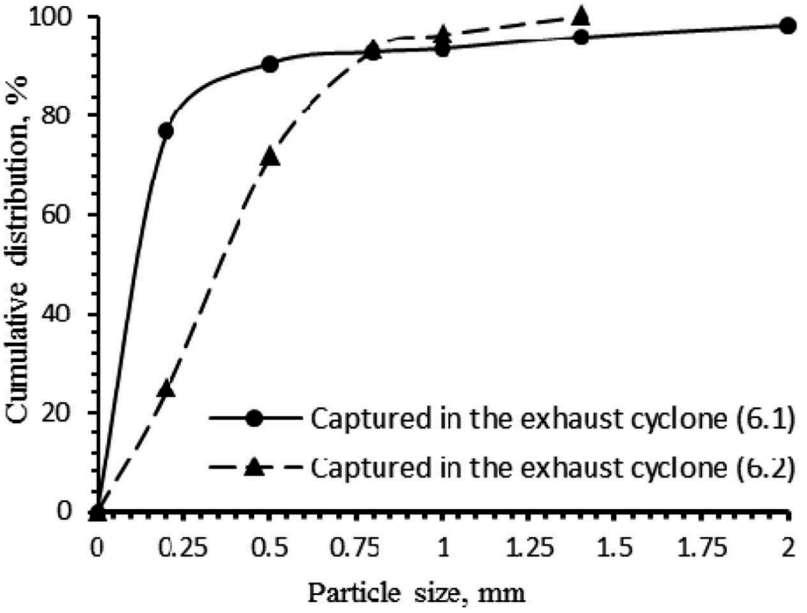

Figure 6. PSD of particles captured in exhaust cyclones (6.1) and (6.2).

Char Particles Characteristics

During the experiments, certain amount of solid material escaped the CFB reactor. This material is essentially fine char particles entrained from the bed. These particles were captured in two exhaust cyclones and taken to the sieve analysis and to the thermogravimetric analysis in order to determine the energy content of the solid phase leaving the reactor. From PSDs of entrained particles shown in Fig. 6 it can be noted that most of the captured particles (80%) have size below 0.2 mm, around 10% between 0.2 mm and 0.75 mm, and 10% particles with size between 0.75 and 2 mm. The existence of large size particles above 0.2 mm in exhaust cyclones can be attributed to the poor performance of CFB cyclone (2) and to difference in coal and char particles density. Char particles similarly to semi-coke particles exhibited swelling due to increased release of volatile. Normally, the PSD of coal injected into a boiler in pulverized coal power plants is significantly smaller than entrained char particles (Beckmann et al. 2016; Vishnoi and Mohapatra 2018). An industrial scale facility will use a more efficient cyclone, which will be effective down to 90 μm and consequently entrained char particles PSD will be comparable with pulverized coal in power plants (Van de Velden et al. 2007). More effective cyclone will also increase the amount of semi-coke produced per kg of input coal.

Table 8 summarizes the results of proximate analysis and the calorific value of char samples captured by exhaust cyclones. As can be seen in this table, the calorific values of entrained char particles varied from 1470 to 1788 kcal/kg and volatile matter from 8.7% to 12.1%. These particles consisted of newly introduced and entrained fine coal and fine char particles formed due to attrition. Even though fine coal particles were small and, therefore, had a smaller temperature gradient, they have not been fully devolatilized due to a short residence time. At the same time, carbon in the worn-down char particles was partially gasified. As a result, fine char particles had higher ash content and lower carbon content compared to semi-coke. Even though, entrained char particles had lower quality than semi-coke in our experiments, entrained char had fixed carbon content higher than char particles in partial gasification experiments conducted by Ye et al. (Ye et al. 2017) and had proximate analysis comparable with semi-coke obtained by Xu et al. (Xu et al. 2018) and by Tang et al. (Tang et al. 2017). In the present study, low ER prevents burnout of fixed carbon and longer residence time improves devolatilization compared to char obtained by Ye et al. (Ye et al. 2017). Char particles volatile matter content correlates with high volatile coal devolatilization experiments in wire mesh reactor (WMR) conducted by Ra et al. (Ra et al. 2014), where fine coal particles devolatilized almost fully at 800–1000°C. However, the residence time in the CFB reactor was shorter for entrained coal particles which escaped the CFB cyclone (2) (3–4 s in CFB and 10 s in WMR). This increased the bulk volatile content of the char captured in exhaust cyclones (6.1 and 6.2).

Effect of Temperature on Syngas Characteristics

Table 9 summarizes the data on the composition of syngas for various operating conditions. During the devolatilization process, coal volatile matter evolves to gases, such as CO, CO_2, CH_4, H_2, and tars (Ra et al. 2014). Taking into account the air velocity, the gas residence time in the reactor was estimated as 3–4 s.

Figure 7(a) illustrates the effect of bed temperature on coal conversion in the reactor. The devolatilization process and burnout of char contribute to the coal conversion. The coal conversion is calculated on the basis of material balance as:

Table 8. Entrained char particles characteristics and yield.

Experiment No		1	2	3	4	5	6	7	8	9	10	11
B_{coal}	kg/h	58	44	65	45	45	55	48	48	40	50	50
$V_{air\ total}$	nm^3/h	110	94	94	112	112	112	65	80	94	107	72
T_{bed}	°C	930	950	930	810	880	990	700	850	780	865	890
$B_{entrained}$	kg/h	13.98	10.98	15.48	11.74	8.86	14.10	13.23	12.10	11.70	13.27	13.31
A_r	%	10.1	8.1	9.5	9.2	8.6	9.7	8.4	9.8	9.5	10.4	11.4
W_r	%	4.6	4.2	5.6	3.8	4	4	3.9	4.7	5	4	3.5
V_r	%	9.4	10.2	8.9	9.3	10.1	12.1	9.4	8.7	9.9	9	8.2
FC_r	%	75.9	77.5	76	77.7	77.3	74.2	78.3	76.8	75.6	76.6	76.9
Entrained char HHV	kcal/kg	1470.7	1566.9	1450.1	1634.7	1242.3	1539.8	1735.3	1557.7	1788.5	1633.8	1642.2

B_{coal}, coal feed mass flow rate; $V_{air\ total}$, total air flow rate; T_{bed}, riser dense-phase-zone temperature; $B_{entrained}$, mass flow rate of char particles entrained from the reactor cyclone (2); A_r, ash content on as received basis; W_r, moisture content; V_r, volatile matter content on as received basis; FC_r, fixed carbon content on as received basis; HHV, higher heating value.

Table 9. Syngas characteristics.

Experiment No		1	2	3	4	5	6	7	8	9	10	11
B_{coal}	kg/h	58	44	65	45	45	55	48	48	40	50	50
$V_{air\ total}$	nm^3/h	110	94	94	112	112	112	65	80	94	107	72
T_{bed}	°C	930	950	930	810	880	990	700	850	780	865	890
CO	Vol %	12.2	10.1	15.1	9.2	7.8	10.2	12.5	13.3	10.9	12.7	14.1
CO_2	Vol %	11.1	9.7	12	8.5	10.2	9.8	12	9.5	7.8	9.3	12.3
H_2	Vol %	4.9	5.2	6.2	4.1	4.3	5.2	5	4.8	5.5	5.1	4.9
O_2	Vol %	1.2	1	0.9	0.6	0.8	1	0.6	0.5	0.6	0.6	0.8
CH_4	Vol %	2.3	1.9	2.6	3.2	2.2	2.2	2.7	2	1.9	2.5	2.4
N_2	Vol %	66.8	70.6	61.7	72.9	73.2	70.1	65.7	68.4	71.8	68.3	64
Syngas HHV	MJ/nm^3	1288.1	1126.6	1560.4	1236.9	1007.1	1181.8	1375.8	1290.9	1184.8	1358.4	1405.1

B_{coal}, coal feed mass flow rate; $V_{air\ total}$, total air flow rate; T_{bed}, riser dense-phase-zone temperature; HHV, higher heating value.

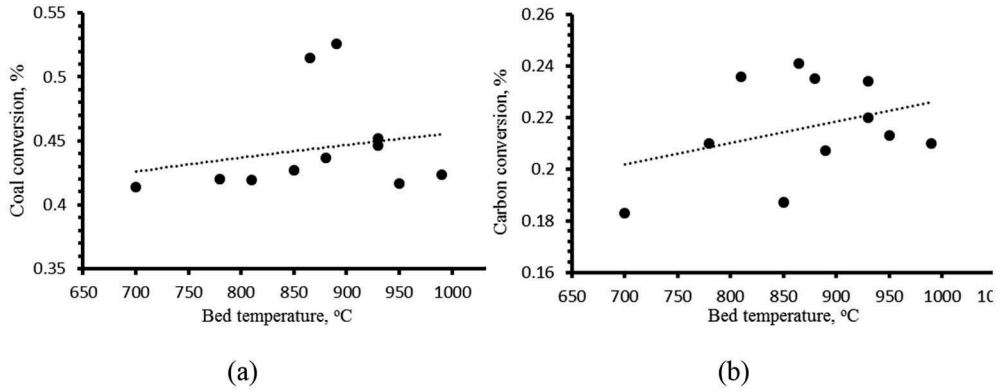

Figure 7. Effect of bed temperature on (a) coal conversion and (b) carbon conversion.

$$C_{coal} = \frac{\left(B_{coal} - B_{bed} - B_{standpipe} - B_{entrained}\right)}{B_{coal}} \times 100\%, \tag{5}$$

where C_{coal} is the conversion of coal to syngas, B_{coal} is the coal feed rate, B_{bed} and $B_{standpipe}$ are the amounts of semi-coke withdrawn from the top of the dense-phase-zone and standpipe, respectively, and $B_{entrained}$ is the amount of entrained char particles captured by the exhaust cyclones (6.1) and (6.2).

Fig. 7(b) shows the carbon conversion at various bed temperatures. The carbon conversion is calculated as:

$$C_{carbon} = \frac{\left(B_{coal}C^{r}_{coal} - B_{char}C^{dry}_{char} - B_{bed}C^{dry}_{bed} - B_{standpipe}C^{dry}_{standpipe}\right)}{B_{coal}C^{r}_{coal} \times 100\%}, \tag{6}$$

where C_{carbon} is the carbon conversion, C^{r}_{coal} and C^{dry}_{char} are the coal carbon content on as received and dry bases, respectively, and C^{dry}_{bed} and $C^{dry}_{standpipe}$ are the carbon content of semi-coke withdrawn from the top of the dense-phase-zone and standpipe on a dry basis, respectively. As can be seen from Fig. 7(a) and Fig. 7(b), the coal and carbon

conversion rates exhibited increasing trends with temperature. Increase of ER increases the burn-out of carbon, therefore low ER keeps fixed carbon gasification low. The release of volatiles, moisture evaporation and conversion of fixed carbon contribute to the rate of coal conversion. In the present work, the coal conversion and carbon conversion rates were deliberately kept low to maximize the semi-coke yield. Coal conversion was kept between 0.42 and 0.52, carbon conversion 0.18 and 0.24. This can be considered low if compared with Ye et al. (Ye et al. 2017) where carbon conversion was varied between 0.79 and 0.88.

Co-generation of Electricity

Table 10 provides information on the yield of semi-coke, physical heat, and calorific value of char and syngas per unit of coal input. The semi-coke yield varied from 0.208 kg to 0.367 kg per kg of coal feed. Thus, even when using the laboratory scale CFB reactor, it was possible to achieve the semi-coke yield of 0.367 kg per 1 kg of coal input at 880°C. Out of 0.367 kg of semi-coke, 0.106 kg of semi-coke was withdrawn from the riser and 0.261 from the loop-seal standpipe. Some 43.6% out of total-fed coal mass was converted to gas and 19.7% was entrained from the bed alongside with the gas as char particles. Entrained char particles contributed 46.40 kcal per kg of coal to the heat that can be utilized in a boiler. At the same time, the char particles had the calorific value 956.1 kcal, which can be utilized in the boiler. The total heat of 1002.5 kcal per kg of coal that char particles can produce in the boiler is the sum of their calorific value and their own heat. Similarly, syngas at 880°C carried the heat equal to 747.7 kcal and the syngas calorific value was 1248.5 kcal per kg of coal. Thus, entrained char particles and syngas can produce 2952.4 kcal per kg of coal heat if combusted in a boiler. In other words, production of 1 ton of semi-coke will consume 2.72 ton of coal, which will produce gas and entrained char products with total heat-carrying 8.04 Gcal. In conventional process, 1 t of semi-coke required 1.65 t of coal and produce coke-oven gas with heat capacity up to 1.91 Gcal (Razzaq, Li, and Zhang 2013). If compared with conventional process, CFB partial gasification semi-coke production can be considered more energy-oriented. As an example, an industrial facility with 100 thousand tons of semi-coke production a year will require 272 thousand tons of Shubarkol coal. Integration of semi-coke plant and a thermal power plant with typical efficiency of 32% (Sarbassov et al. 2013) will be able to produce 300 GWh of power annually.

Semi-coke Intrinsic Properties

X-ray diffraction is a powerful tool for determination of crystalline characteristics of carbonaceous materials, including coal, semi-coke, and coke (Lu et al. 2001). Figure 8 represents the XRD curves of the semi-coke produced during the experiments at various CFB reactor temperatures. The vertical axis represents intensity of the diffraction peaks. The horizontal axis represents 2-θ scattering angle. The 2-θ band (002) at around 26° is considered as the carbon peak. Semi-coke samples in this study have both amorphous and hexagonal crystalline structure carbon. The semi-coke crystallite size was determined using the Scherrer equation (Xu et al. 2018):

Table 10. Semi-coke yield, physical heat and calorific value of char and syngas available for power generation.

Experiment No		1	2	3	4	5	6	7	8	9	10	11
B_{coal}	kg/h	58	44	65	45	45	55	48	48	40	50	50
$V_{air\ total}$	nm^3/h	110	94	94	112	112	112	65	80	94	107	72
T_{bed}	°C	930	950	930	810	880	990	700	850	780	865	890
Quantity of semi-coke from 1 kg of input coal	kg/kg coal	0.307	0.334	0.315	0.320	0.367	0.320	0.310	0.321	0.288	0.220	0.208
Heat of particles entrained from the bed	kcal/kg coal	33.51	47.92	28.31	42.73	46.40	45.48	40.49	37.47	51.17	37.21	33.90
Heat of syngas per 1 nm3	$kcal/nm^3$	289.90	300.12	286.75	246.64	278.37	304.09	205.10	258.09	233.53	261.62	271.97
Heat of syngas from 1 kg of input coal	kcal/kg of coal	650.23	717.44	530.95	665.22	747.71	697.87	333.97	496.81	603.83	647.58	483.42
Calorific value of char per 1 kg of input coal	kcal/kg of coal	1134.3	1203.5	1053.4	1298.6	956.1	1203.6	1381.8	1216.7	1420.4	1436.0	1420.7
Calorific value of syngas per kg of input coal	kcal/kg of coal	1155.9	1205.3	1130.9	1032.4	1248.5	868.7	3228.5	3256.9	3189.8	3822.8	3731.2
Total heat to boiler per kg of coal	kcal/kg of coal	2940.4	3126.2	2715.2	2996.3	2952.4	2770.2	4944.2	4970.4	5214.1	5906.4	5635.4

B_{coal}, coal feed mass flow rate; $V_{air\ total}$, total air flow rate; T_{bed}, riser dense-phase-zone temperature.

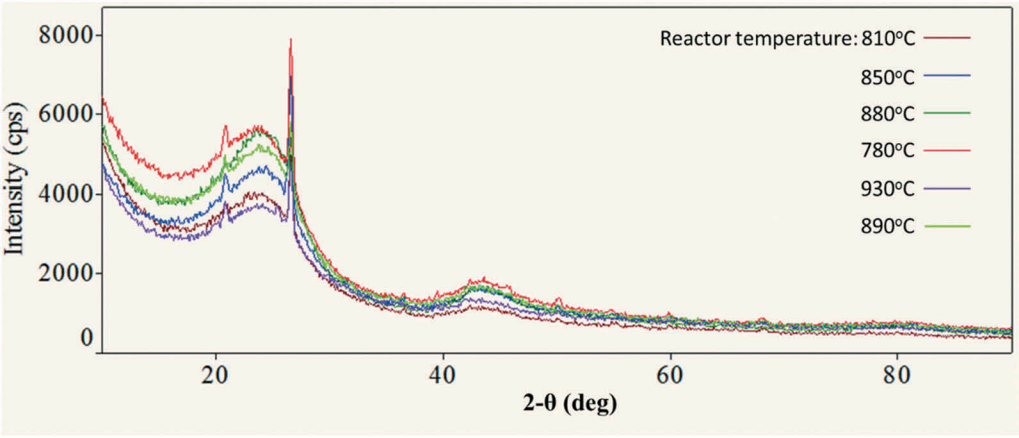

Figure 8. X-ray diffraction curves of semi-coke produced.

$$L_C = \frac{0.89\lambda}{\beta cos\theta} \tag{7}$$

where L_C is the crystallite size, d is the interlayer spacing of the crystalline structure, θ is the diffraction angle, λ is X-ray wavelength (Å) which is equal to 1.54051 for Cu-Kα, and β is the full width at half maximum (FWHM) intensity of the peak.

Table 11 summarizes the XRD results for seven samples from the current study as well as results by Xu et al. on dissolution kinetics of semi-coke and coke in COREX gasifier (Xu et al. 2018). The partial gasification semi-coke has substantially larger crystalline size, compared to XRD results obtained by Xu et al. (Xu et al. 2018). They concluded that the increase in microcrystalline order degree enhances the dissolution rate in COREX gasifiers. Therefore, semi-coke produced in partial gasification

Table 11. Semi-coke samples XRD analysis results.

Experiment No.	Experiment temperature	Diffraction angle	Interlayer distance	Height	FWHM	Crystallite size	Reactivity
	°C	2θ, deg	d, Å	n, counts	β, deg	L_C, Å	R_o, $10^{-6}s^{-1}$
9	780	26.57	3.352	2277	0.36	236	7.57
4	810	26.524	3.3578	413	0.20	436	7.70
8	850	26.638	3.3437	1297	0.294	290	7.05
5	880	26.589	3.350	2322	0.321	266	7.14
11	890	26.566	3.3526	10452	0.341	250	7.34
3	930	26.530	3.357	440	0.37	231	6.11
2	950	26.571	3.352	2208	0.361	236	6.97
Lump coal [38]	-	24.58	3.6	2.14	10.37	7.8	-
Semi-coke [38]	-	25.02	3.6	2.58	8.76	9.2	-
Coke [38]	-	26.31	3.4	6.81	3.50	23.1	-

FWHM, full width at half maximum intensity of the peak.

process is expected to have higher carbon dissolution rate in COREX process compared to semi-coke produced in conventional coke-ovens.

Metal oxides present in the coal ash have certain catalytic effect on gasification reactions occurring in blast furnaces and COREX units. Mainly these metal oxides are iron, calcium,

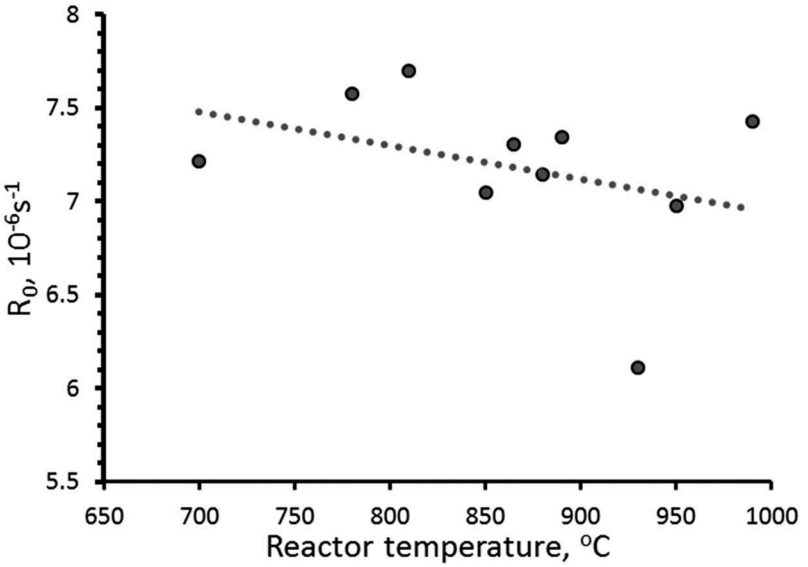

Figure 9. Expected reactivity of semi-coke.

potassium, and sodium. Expected catalytic effect is designated as catalytic index (*CI*). Based on the ash composition the catalytic index can be estimated using the equation:

$$CI = [Fe_2O_3] + [CaO] + [K_2O] + [Na_2O] = 12.9\% \tag{8}$$

Zhang investigated the correlation of coke reactivity and critical coke properties using thermogravimetric method and simulating conditions similar to blast furnace (Zhang 2018). Zhang simulated isothermal conditions occurring in a blast furnace using a furnace and determined carbon conversion of five cokes at 1273°C. Zhang came to a conclusion that coke initial reactivity at 1273°C reactivity is in correlation with catalytic index (*CI*), ash content, crystalline size, and Brunauer–Emmett–Teller (BET) surface area. BET surface area effect was insignificant compared to other three factors. Cham et al. compared carbon dissolution of two cokes made from coals of similar rank, ash yield and carbon crystallite structural parameters, and came to a conclusion that the most influential factor is coal ash catalytic characteristic (Cham et al. 2004). According to Zhang coke reactivity R_0 empirically correlate with coke intrinsic properties according to the following equation (Zhang 2018):

$$R_0 = 49.9 * L_c^{-0.39} * \exp[-9.48 * A * (1 - CI)] \tag{9}$$

where L_C is the carbon crystalline size, A is the ash content of semi-coke, and CI is the semi-coke catalytic index. Figure 9 represents the trendline for correlation between the expected semi-coke reactivity in blast furnace and CFB partial gasification process temperature. The expected reactivity was calculated using Equation 9 (Zhang 2018), semi-coke reactivity similar to Ye et al. findings (Ye et al. 2017)

Conclusion

The feasibility of char production for use as a metallurgical semi-coke and the potential to integrate the semi-coke production process with a thermal power plant have been evaluated for a circulating fluidized bed reactor. The laboratory-scale CFB reactor system was constructed and the partial gasification of the fine fraction of Shubarkol coal was carried out at various coal feed rates and air-to-fuel equivalence ratios.

As a result, this study experimentally proved the feasibility of a novel semi-coke production approach involving partial gasification of coal in CFB. The process is sensitive to the riser bed temperature, where with increasing temperature, the output of semi-coke volatiles content decreases. Experiments demonstrated that the process is autothermal and do not require outside inputs of energy during operation. At temperatures above 850°C, output semi-coke has 3–6% of volatiles and more than 80% of the fixed carbon content in all experiments. On average, it was possible to produce 300–350 kg of semi-coke per ton of coal input in the laboratory scale process. The process has been optimized to produce 0.367 kg of semi-coke per kg of input coal. However, depending on the input coal characteristics and CFB unit size the semi-coke output can be increased. Semi-coke is suitable for silicomanganese production and blast furnace injection. Syngas and char entrained away from the reactor have the considerable potential for power co-production. In case of industrial facility with output of 100 thousand tons of semi-coke per year, the integrated power plant can produce additional 300 GWh of power per year.

Semi-coke XRD analysis revealed that its crystalline size is considerable larger than reference case from the literature. Partial gasification semi-coke can be used for blast furnace injection. Semi-coke reactivity and the CFB partial gasification temperature have negative correlation.

Acknowledgments

The authors thank Eurasian Resources Group for funding the circulating fluidized bed reactor construction in Nazarbayev University.

References

Alauddin, Z., A. B. Zainal, P. Lahijani, M. Mohammadi, and A. R. Mohamed. 2010. Gasification of lignocellulosic biomass in fluidized beds for renewable energy development: A review. *Renewable and Sustainable Energy Reviews* 14(9):2852–62. Elsevier Ltd. doi:10.1016/j.rser.2010.07.026.

American Iron and Steel Institute. 2010. "Technology roadmap research progam."

Basu, P. 1999. "Combustion of coal in circulating fluidized-bed boilers: A review." *Chemical Engineering Science* 54(22): 5547–5557. doi:10.1016/S0009-2509(99)00285-7.

Beckmann, A. M., M. Mancini, R. Weber, S. Seebold, and M. Müller. 2016. Measurements and CFD modeling of a pulverized coal flame with emphasis on ash deposition. *Fuel* 167: Elsevier Ltd: 168–79. doi:10.1016/j.fuel.2015.11.043.

Borah, R. C., P. Ghosh, and P. G. Rao. 2011. A review on devolatilization of coal in fluidized bed. *International Journal of Energy Research* 35(April): 929–963. doi:10.1002/er.1833.

Brunauer, S., P. H. Emmett, and E. Teller. 1938. Adsorption of gases in multimolecular layers. *Journal of the American Chemical Society* 60 (2):309–19. doi:10.1021/ja01269a023.

Cham, S. T., V. Sahajwalla, R. Sakurovs, H. Sun, and M. Dubikova. 2004. Factors influencing carbon dissolution from cokes into liquid iron. *ISIJ International* 44 (11):1835–41. doi:10.2355/isijinternational.44.1835.

Chen, G., Y. Zhang, J. Zhu, Y. Cao, and W. Pan. 2011. Coal and biomass partial gasification and soot properties in an atmospheric fluidized bed. *Energy and Fuels* 25 (5):1964–69. doi:10.1021/ef101754v.

Commitee of technical requilation and metrology, Ministry of industry and new technologies, Republic of Kazakhstan. 2011. "STRK 2145-2011 coke made at medium temperature from kazakhstan coals. General technical requirements."

Dai, B., J. F. Lei Zhang, A. H. Cui, and L. Zhang. 2017. Integration of pyrolysis and entrained-bed gasification for the production of chemicals from victorian brown coal — process simulation and exergy analysis. *Fuel Processing Technology* 155: Elsevier B.V.: 21–31. doi:10.1016/j.fuproc.2016.02.004.

Fushimi, C., S. Okuyama, M. Kobayashi, M. Koyama, and H. Tanimura. 2017. Pyrolysis of low-rank coal with heat-carrying particles in a downer reactor. *Fuel Processing Technology* 167: Elsevier B.V.: 136–45. doi:10.1016/j.fuproc.2017.06.029.

2002. GOST 9326-2002 solid mineral fuels – determination of chlorine. Minsk.

2012. GOST R 54251 coke — determination of bulk density in a small container (ISO 567:1995). Moscow: Standartinform. doi:10.1094/PDIS-11-11-0999-PDN

Guo, Z., Q. Wang, M. Fang, Z. Luo, and K. Cen. 2014. Thermodynamic and economic analysis of polygeneration system integrating atmospheric pressure coal pyrolysis technology with circulating fluidized bed power plant. *Applied Energy* 113: Elsevier Ltd: 1301–14. doi:10.1016/j.apenergy.2013.08.086.

Hasanbeigi, A., M. Arens, and L. Price. 2014. Alternative emerging ironmaking technologies for energy-efficiency and carbon dioxide emissions reduction: A technical review. *Renewable and Sustainable Energy Reviews* 33:645–58. doi:10.1016/j.rser.2014.02.031.

He, K., and L. Wang. 2017. A review of energy use and energy-efficient technologies for the iron and steel industry. *Renewable and Sustainable Energy Reviews* 70 (December 2016):1022–39. Elsevier Ltd. doi:10.1016/j.rser.2016.12.007.

Hu, L., J. Hongguang, G. Lin, and H. Wei. 2011. Techno-economic evaluation of coal-based polygeneration systems of synthetic fuel and power with CO2 recovery. *Energy Conversion and Management* 52 (1):274–83. Elsevier Ltd. doi:10.1016/j.enconman.2010.06.068.

IEA. 2017. Southeast Asia energy outlook 2017. 149. doi:10.1787/weo-2013-en.

Jing, X., Z. Zhu, P. Dong, G. Meng, K. Wang, and Q. Lyu. 2017. Energy quality factor and exergy destruction processes analysis for a proposed polygeneration system coproducing semicoke, coal gas, tar and power. *Energy Conversion and Management* 149:52–60. Elsevier Ltd. doi:10.1016/j.enconman.2017.07.014.

Korshenko, V. S., S. P. Kim, S. V. Nechipurenko, S. A. Yefremov, and M. K. Nauryzbayev. 2016. Diversification of JSC 'Shubarkol Komir' production with obtaining products of coal deep processing. 567–68. doi:10.1007/978-3-319-40943-6.

Kumar, P. S., B. M. Ranjan, S. Ghosh, and V. V. S. Raju. 2008. Maximisation of non-coking coals in coke production from non-recovery coke ovens. *Ironmaking & Steelmaking* 35 (1):33–37. doi:10.1179/174328107X174762.

Kunii, D., and O. Levenspiel. 1997. Circulating fluidized-bed reactors. *Chemical Engineering Science* 52 (15):2471–82. doi:10.1016/S0009-2509(97)00066-3.

Li, K., R. Khanna, J. Zhang, Z. Liu, V. Sahajwalla, T. Yang, and D. Kong. 2014a. The evolution of structural order, microstructure and mineral matter of metallurgical coke in a blast furnace: A review. *Fuel* 133 (30):194–215. doi:10.1016/j.fuel.2014.05.014.

Li, Q., X. Li, J. Jiang, L. Duan, S. Ge, Q. Zhang, J. Deng, S. Wang, and J. Hao. 2016. Semi-coke briquettes: towards reducing emissions of primary PM 2.5, particulate carbon, and carbon monoxide from household coal combustion in China. *Scientific Reports* 6 (June 2015):1–10. doi:10.1038/srep19306.

Li, Y., G. Zhang, Y. Yang, D. Zhai, K. Zhang, and X. Gang. 2014b. Thermodynamic analysis of a coal-based polygeneration system with partial gasification. *Energy* 72:201–14. doi:10.1016/j.energy.2014.05.025.

Lu, L., V. Sahajwalla, C. Kong, and D. Harris. 2001. Quantitative X-Ray diffraction analysis and its application to various coals. *Carbon* 39 (12):1821–33. doi:10.1016/S0008-6223(00)00318-3.

Menéndez, J. A., R. Álvarez, and J. J. Pis. 1999. Determination of metallurgical coke reactivity at INCAR: NSC and ECE-INCAR reactivity tests. *Ironmaking & Steelmaking* 26 (2):117–21. doi:10.1179/030192399676997.

Nowak, W., and P. Mirek. 2013. Circulating Fluidized Bed Combustion (CFBC). In Fabrizio Scala (Ed.), *Fluidized bed technologies for near-zero emission combustion and gasification*. Sawston, Cambridge: Woodhead Publishing Limited. doi: 10.1533/9780857098801.3.701.

Pan, S., S. Hui, L. Liang, C. Liu, L. Congxin, and X. Zhang. 2015. Weight loss and tar evolution during coal devolatilization at various heating rates. *Energy and Fuels* 29 (2):520–29. doi:10.1021/ef502031v.

Ra, H. W., M. W. Seo, S. J. Yoon, S. M. Yoon, J. K. Kim, J. G. Lee, and S. B. Park. 2014. Devolatilization characteristics of high volatile coal in a wire mesh reactor. *Korean Journal of Chemical Engineering* 31 (9):1570–76. doi:10.1007/s11814-014-0061-z.

Razzaq, R., L. Chunshan, and S. Zhang. 2013. Coke oven gas: availability, properties, purification, and utilization in China. *Fuel* 113:287–99. Elsevier Ltd. doi:10.1016/j.fuel.2013.05.070.

Sarbassov, Y., A. Kerimray, D. Tokmurzin, G. C. Tosato, and R. De Miglio. 2013. Electricity and heating system in Kazakhstan: Exploring energy efficiency improvement paths. *Energy Policy* 60:431–44. doi:10.1016/j.enpol.2013.03.012.

Sermin, G. Z., J. R. Gibbins, I. E. Katheklakis, and R. Kandiyoti. 1990. Comparison of coal pyrolysis product distributions from three captive sample techniques. *Fuel* 69 (3):383–90. doi:10.1016/0016-2361(90)90104-X.

Song, H., G. Liu, and W. Jinhu. 2016. Pyrolysis characteristics and kinetics of low rank coals by distributed activation energy model. *Energy Conversion and Management* 126:1037–46. doi:10.1016/j.enconman.2016.08.082.

Strakhov, V. M. 2009. Alternative carbon reducing agents for ferroalloy production. *Coke and Chemistry* 52 (1):19–22. doi:10.3103/S1068364X09010062.

Street, S., G. Brooks, L. Reilly, and H. K. Worner. 1998. EnvIRONment and other bath smelting processes for treating organic and ferrous wastes. *The Journal of the Minerals, Metals & Materials Society (TMS)* 50 (4):43–47. doi:10.1007/s11837-998-0268-8.

Svyatov, B. A., V. M. Strakhov, and I. V. Surovtseva. 2012. Semicoke production from long-flame coal in a rotary furnace. *Coke and Chemistry* 55 (6):231–35. doi:10.3103/S1068364X12060075.

Tang, Q., J. Zhang, J. Zhong, L. Kejiang, B. Gao, Z. Wang, X. Runsheng, G. Wang, and Z. Liu. 2017. Utilization of semi-coke in iron making technologies in China. *Metallurgical Research & Technology* 114 (4):403. doi:10.1051/metal/2017031.

Taylor, R. 2000. 4.13 – Carbon matrix composites. *Comprehensive Composite Materials* 387–426. doi:10.1016/B0-08-042993-9/00100-5.

Trubetskaya, A., P. A. Jensen, A. D. Jensen, A. D. Garcia Llamas, K. Umeki, and P. Glarborg. 2016. Effect of fast pyrolysis conditions on biomass solid residues at high temperatures. *Fuel Processing Technology* 143: Elsevier B.V.: 118–29. doi:10.1016/j.fuproc.2015.11.002.

Van de Velden, M., J. Baeyens, B. Dougan, and M. Alan. 2007. Investigation of operational parameters for an industrial CFB combustor of coal, biomass and sludge. *China Particuology* 5 (4):247–54. doi:10.1016/j.cpart.2007.05.001.

Vishnoi, N., and S. K. Mohapatra. 2018. Study of particle size distribution of pulverized coals in utility boilers. *Particulate Science and Technology* 36 (8):999–1005. Taylor & Francis. doi:10.1080/02726351.2017.1334731.

Wootten, J. M., M. Nawaz, R. G. Duthie, R. A. Knight, M. Onischak, P. Babu, and W. G. Bair. 1988. "Literature survey of mild gasification processes, co-products upgrading and utilization, and market assessment."

World Coal Institute. 2007. Coal & steel. *World Coal Institute*. doi:10.1094/PDIS-91-4-0467B

World steel Association. 2018. Coal & steel. *World Steel in Figures 2018. Brussels*.

Wu, C., and V. Sahajwalla. 2014. Dissolution rates of coals and graphite in Fe-C-S melts in direct ironmaking: Dependence of carbon dissolution rate on carbon structure. *Mineralogical Magazine* 78 (5):1161–75. doi:10.1180/minmag.2014.078.5.05.

Wu, Z., W. Yang, X. Tian, and B. Yang. 2017b. Synergistic effects from co-pyrolysis of low-rank coal and model components of microalgae biomass. Energy Conversion and Management 135: Elsevier Ltd: 212–25. doi:10.1016/j.enconman.2016.12.060.

Xu, C., and Q. Cang. 2010. A brief overview of low CO2 emission technologies for iron and steel making. *Journal of Iron and Steel Research International* 17 (3):1–7. Central Iron and Steel Research Institute. doi:10.1016/S1006-706X(10)60064-7.

Xu, R. S., J. L. Zhang, W. Wang, H. B. Zuo, Z. L. Xue, and M. M. Song. 2018. Dissolution kinetics of solid fuels used in COREX gasifier and its influence factors. *Journal of Iron and Steel Research International* 25 (3):298–309. Springer Singapore. doi:10.1007/s42243-018-0030-6.

Xu, Y., G. Zang, H. Chen, B. Dou, and C. Tan. 2012. Co-production system of hydrogen and electricity based on coal partial gasification with CO2 capture. *International Journal of Hydrogen Energy* 37 (16):11805–14. Pergamon. doi:10.1016/J.IJHYDENE.2012.05.037.

Yang, W.-C. 2003. Handbook of fluidization and fluid-particles systems. *Chemical engineering*. New York: Taylor & Francis. doi:10.1016/S1672-2515(07)60126-2.

Ye, C., Q. Wang, Y. Lifeng, Z. Luo, and K. Cen. 2018. Characteristics of coal partial gasification experiments on a circulating fluidized bed reactor under CO2–O2atmosphere. *Applied Thermal Engineering* 130: Elsevier Ltd: 814–21. doi:10.1016/j.applthermaleng.2017.11.071.

Ye, C., Q. Wang, Z. Luo, K. Jin, G. Xie, M. Siyil, and K. Cen. 2017. Characteristics of coal partial gasification on a circulating fluidized bed reactor. *Energy & Fuels* 31:2557–64. doi:10.1016/j.applthermaleng.2017.11.071.

Yi, Q., J. Feng, L. Bingchuan, J. Deng, Y. Changlian, and L. Wenying. 2013. Energy evaluation for lignite pyrolysis by solid heat carrier coupled with gasification. *Energy and Fuels* 27 (8):4523–33. doi:10.1021/ef400865h.

Yu, J., V. Strezov, J. Lucas, and T. Wall. 2003. Swelling behaviour of individual coal particles in the single particle reactor. *Fuel* 82 (15–17):1977–87. doi:10.1016/S0016-2361(03)00159-5.

Zhang, H. 2018. Relationship of coke reactivity and critical coke properties. *Metallurgical and Materials Transactions B* Springer US. doi:10.1007/s11663-018-1438-x.

Zhu, D. Q., Y. H. Luo, J. Pan, and X. L. Zhou. 2015. Characterization of semi-coke generated by coal-based direct reduction process of siderite. *Journal of Central South University* 22 (8):2914–21. doi:10.1007/s11771-015-2826-x.